Kinematic Precise Point Positioning at Remote Marine Platforms

J Geng, FN Teferle, X Meng, AH Dodson
Institute of Engineering Surveying and Space Geodesy, the University of Nottingham, NG7 2RD, UK

Abstract: Precise kinematic differential positioning using the Global Positioning System (GPS) at a marine platform usually requires a relatively short distance (e.g. <500 km) to a land-based reference station. As an alternative, precise point positioning (PPP) is normally considered free from this limiting requirement. However, due to the prerequisite of network-based satellite products, PPP at a remote marine platform may still be affected by its distance to the reference network. Hence, this paper investigates this scenario by configuring rings of reference stations with different radii centered on a to-be-positioned marine platform. Particularly, we applied ambiguity resolution at a single station to PPP by estimating uncalibrated phase delays (UPDs). We used three rings of reference stations centered on a vessel, with radii of roughly 900 km, 2000 km and 3600 km, to determine satellite clocks and UPDs independently. For comparison, we also performed differential positioning based on a single reference station with baseline lengths of about 400 km, 1700 km and 2800 km. We demonstrate that, despite the increasing ring-network radius to a few thousand kilometers, the overall change in accuracy of the satellite clocks that are used at the vessel is smaller than 0.02 ns, and the RMS values of differences between the three sets of narrow-lane UPD estimates are around 0.05 cycles only. Moreover, the kinematic positioning accuracy of PPP is affected by the increasing ring-network radius, but can still achieve several centimeters after ambiguity resolution when the vessel is over a few thousand kilometers away from the ring network, showing better performance than that of differential positioning. Therefore, we propose that ambiguity-fixed PPP can be used at remote marine platforms that support precise oceanographic and geophysical applications in open oceans.

Keywords: Precise point positioning; Ambiguity resolution; Kinematic; Marine; Open oceans

1 INTRODUCTION

Marine geodesy is usually related to the highly precise kinematic positioning of surveying platforms such as vessels, buoys and aircrafts. These derived positions can be critical to oceanography, e.g. in measuring tidal variation, and to seafloor geophysics, e.g. in estimating underwater plate movement, since most tectonic boundaries and deformation zones are located under oceans and cannot be observed directly (Spiess et al. 1998). Currently, the Global Positioning System (GPS) can provide a kinematic positioning accuracy of decimeter to centimeter level in post-processing mode in a global reference frame, thus it is considered very appropriate in determining marine platform positions. For instance, GPS can be combined with acoustic ranging instruments on a vessel to locate seafloor geodetic markers and detect the

seafloor crustal deformation (Chadwell and Spiess 2008; Gagnon et al. 2005); GPS positioning of a buoy can be used to measure the ocean wave and tidal height for satellite altimeter calibration, mean sea level determination, and even tsunami monitoring (Kato et al. 2005; Watson 2005); and airborne GPS combined with a light detection and ranging system can be used to map sea surface and measure ice roughness (Han and Rizos 2000; Rivas et al. 2006).

Most of these offshore applications employ differential GPS positioning techniques, and thus relatively short baselines are preferable. Vessels used for seafloor geodesy are typically less than 500 km away from shores, and buoys supporting altimeter calibration are usually within 20 km of an onshore reference station (Chadwell and Bock 2001). Such baseline lengths can only cover a minimal margin of the vast oceanic areas, confining the oceanographic and geophysical research to inshore areas. Therefore, kinematic GPS positioning, providing an accuracy of a few centimeters for ultra long-range (e.g. >1000 km) marine platforms, is an indispensible prerequisite for future oceanographic and geophysical applications in open oceans (Fell and Maul 2000). However, differential GPS positioning suffers from the so-called baseline length problem, i.e. the positioning accuracy deteriorates with the increased baseline length. The total de-correlation between the atmospheric delays at two ultra distant stations poses a great challenge for reliable ambiguity resolution (e.g. Colombo et al. 2001). In this case, ambiguity resolution is sometimes ignored. Consequently, usually only decimeter-level kinematic positioning accuracy is achievable over ultra long baselines (Teunissen and Kleusberg 1997). Additionally, due largely to logistical expenses, it is usually infeasible for ultra long-range differential positioning to employ multiple reference stations around a to-be-positioned station, although this can lead to more reliable and accurate positioning (Teunissen and Kleusberg 1997). Hence, in this study, differential positioning corresponds to only one reference station, except when otherwise noted.

In the past decade, precise point positioning (PPP) has been developed in which un-differenced observations at only a single user station are processed to obtain decimeter- to millimeter-level positioning accuracy when precise satellite orbits and clocks are provided (Zumberge et al. 1997). Hence, it is normally recognized that PPP is free from the constraint of baseline lengths, suggesting an efficient and cost-effective solution for highly precise kinematic positioning of marine platforms. Actually, kinematic PPP can achieve decimeter-level or even centimeter-level positioning accuracy for only one ice-borne or airborne GPS receiver (Zhang and Andersen 2006; Zhang and Forsberg 2007).

Nevertheless, the satellite clocks supporting PPP have to be determined using a network of land-based reference stations, implying that PPP may also be subject to the distance between the network and the user station. This issue is critical for

marine platforms located in the central open oceans where the nearest reference station might be a few thousand kilometers away. We indicate that, due largely to the dynamic smoothing in the orbit determination, a homogeneous GPS orbit accuracy at centimeter level can be obtained within a continuous daily arc (Griffiths and Ray 2009), showing that the possible orbit accuracy deterioration over the vast oceanic areas is minimal and is thus ignored in this study. Particularly, ambiguity resolution is normally ignored at a single station in PPP due to non-integer uncalibrated phase delays (UPDs) which can hardly be separated from integer ambiguities in a least squares adjustment (Ge et al. 2008). This shortcoming limits the further positioning accuracy improvement of PPP. Fortunately, recent studies have shown that the integer property of ambiguities can be recovered if the UPDs are precisely determined in advance using a network of reference stations (Ge et al. 2008; Laurichesse and Mercier 2007). Geng et al. (2009) showed that the UPDs derived from a regional network can be effectively used for ambiguity resolution at a remote static station which is a few thousand kilometers away, showing a great potential for ambiguity resolution at mobile marine platforms in open oceans.

This paper aims at assessing the accuracy of network-based satellite clock and UPD estimates when they are applied to the positioning of a remote marine platform. The kinematic PPP performance is compared with that of kinematic long-range differential positioning, when ambiguity resolution is applied to both techniques. In the following Section 2 introduces the methods adopted for kinematic PPP and differential positioning with ambiguity resolution; Section 3 introduces the data and models used in this study; Section 4 includes the results and discussions on the vessel-borne data processing; and Section 5 draws the conclusions.

2 METHODS

Both kinematic PPP and long-range differential GPS techniques are introduced in this section, including data processing strategies and ambiguity resolution methods.

2.1 PPP WITH AMBIGUITY RESOLUTION

We configured three rings of reference stations centered on a marine platform to simulate its possible location in open oceans. The ring radius is defined as the mean distance between each reference station and the marine platform. All ring networks do not overlap each other, and each provides independent satellite clock and UPD estimates for the kinematic PPP. Additionally, we expect that the quality of these satellite products used at the central platform, is mainly subject to

its nearest surrounding reference stations. This explains why in this study we used only rings of reference stations, rather than a global network. Moreover, we estimated epoch-wise satellite clocks by fixing the known satellite orbits, and UPDs by fixing the orbits and the estimated satellite clocks.

Ambiguity resolution in PPP is divided into two stages, namely the network solution and the point solution (Geng et al. 2009). For the network solution, UPDs are determined by averaging the fractional parts of all involved between-satellite-difference (BSD) ambiguity estimates at reference stations. For the point solution, the BSD UPDs are used to recover the integer property of BSD ambiguity estimates at a single station. We indicate that these BSD UPDs are merely the fractional parts of the real ones, as the integer parts can be assimilated into integer ambiguities without impairing the PPP performance. For brevity, 'BSD UPD' is hereafter called 'UPD'. For this PPP solution, we used the PANDA (Positioning And Navigation Data Analyst) software (Shi et al. 2008).

For the network solution, the UPDs include both wide-lane and narrow-lane ones. The wide-lane UPD $\phi_w^{i,j}$ between satellite i and j is determined by

$$\phi_w^{i,j} = \left\langle \left[b_{wk}^{i,j} \right] - b_{wk}^{i,j} \right\rangle \tag{1}$$

where $b_{wk}^{i,j}$ denotes a wide-lane BSD ambiguity estimate derived from Melbourne-Wübbena combination observations at station k (see Melbourne 1985); $[\cdot]$ denotes the integer part of $b_{wk}^{i,j}$; and $\langle \cdot \rangle$ denotes the averaging over all involved fractional parts. Wide-lane UPDs can be very stable within at least several days (Ge et al. 2008). Once $\phi_w^{i,j}$ is obtained, wide-lane BSD ambiguities can be fixed to integers, and the narrow-lane UPD $\phi_n^{i,j}$ is determined by

$$\phi_n^{i,j} = \left\langle \left[\frac{f_1 + f_2}{f_1} b_{ck}^{i,j} - \frac{f_2}{f_1 - f_2} n_{wk}^{i,j} \right] - \frac{f_1 + f_2}{f_1} b_{ck}^{i,j} + \frac{f_2}{f_1 - f_2} n_{wk}^{i,j} \right\rangle \tag{2}$$

where f_1 and f_2 denote the L1 and L2 frequencies, respectively; $b_{ck}^{i,j}$ denotes the real-valued BSD ambiguity estimate for the ionosphere-free observable; and $n_{wk}^{i,j}$ denotes the integer wide-lane BSD ambiguity estimate. Due to the instability of long-term narrow-lane UPD estimates, their determination is of major concern and thus the method proposed by Geng et al. (2009), in which one narrow-lane UPD is estimated within each full pass of a satellite pair over a regional network, is adopted in this study. In addition, we required that at least five reference stations should observe a satellite pair during its one pass, otherwise its narrow-lane UPD estimate is not used.

For the point solution, wide-lane and narrow-lane BSD ambiguity resolution can be attempted sequentially by introducing the above UPD corrections into the BSD ambiguity estimates at a single station. In this study, the integer resolution of wide-lane and narrow-lane BSD ambiguities follows the sequential bias fixing strategy (Dong and Bock 1989).

2.2 LONG-RANGE DIFFERENTIAL POSITIONING

Corresponding to the three ring networks in Section 2.1, we selected three reference stations with different distances to a marine platform to attempt the long-range kinematic differential positioning. Considering the de-correlation of atmospheric delays between two distant stations, we have to use ionosphere-free observations to eliminate the first-order ionospheric delays, and the residual zenith tropospheric delays have to be estimated at both stations. In addition, using precise satellite orbits is also mandatory for ultra long baselines. For this differential positioning, we used Bernese GPS Software 5.0 (Dach et al. 2007).

As recommended by Dach et al. (2007), double-difference (DD) ambiguity resolution for ultra long baselines consists of two steps. In the first step, wide-lane DD ambiguities are fixed to integers using Melbourne-Wübbena combination observations. In the second step, narrow-lane DD ambiguities are computed using the integer wide-lane DD ambiguities and the DD ambiguity estimates derived from the ionosphere-free observations. Narrow-lane DD ambiguity resolution is then attempted to generate the ambiguity-fixed solutions. Thus this method actually highly resembles that for PPP ambiguity resolution, except for the UPD issue. The sigma-dependent bias fixing strategy is adopted for the integer resolution of wide-lane and narrow-lane DD ambiguities.

3 DATA AND MODELS

A vessel-borne 1-Hz GPS data set was collected in the Bohai Sea of China on November 27th in 2004, covering over six hours from about 1:37:00 am to around 7:53:00 am (UTC), during which the vessel sailed for more than 250 km at a mean velocity of approximately 10 m/s. Three 1-Hz reference stations, i.e. REF1, REF2 and REF3, were established around this vessel. Figure 1 shows the vessel trajectory and the baseline lengths between the 1-Hz reference stations.

The truth benchmark for the vessel-borne antenna positions is obtained by differential positioning with the three 1-Hz reference stations using Bernese GPS software 5.0. We applied an integrated adjustment of the three kinematic baselines, and estimated residual zenith tropospheric delays. For the resulting ambiguity-fixed position estimates, we believe that their horizontal accuracy is better than 5 cm, and vertical around 5 cm (e.g. Grejner-Brzezinska et al. 2005). Moreover, for efficiency, we only obtained a position estimate every 5 s.

Figure 2 shows the distribution of reference stations used for the satellite clock and UPD determination. The blue dots, brown triangles and black inverted triangles denote three rings of reference stations centered on the vessel with radii of roughly 900 km, 2000 km and 3600 km, respectively. For brevity, they are hereafter called the small, medium, and large ring networks, which consist of 8, 17 and 14 stations, respectively. All reference stations are from the International GNSS Service (IGS) permanent network with daily GPS data of a 30-second interval. We indicate that the three ring networks were used independently, and daily data were processed in this study. In addition, the station BJFS, TWTF and PIMO are used as the reference stations in the differential positioning, and their distances from the vessel are approximately 400 km, 1700 km and 2800 km, respectively (Figure 2). More than seven satellites per epoch were available on average at these three reference stations during the vessel-borne data collection.

Kinematic PPP and differential positioning employ almost the same data modeling. We used the satellite orbits, Earth rotation parameters, and the P1-C1 differential code biases from the Center for Orbit Determination in Europe (CODE). Moreover, we applied the relative antenna phase centers and the phase wind-up corrections to keep consistence with the CODE products in 2004 (Gendt and Nischan 2005). A cut-off angle of 7° is set for usable observations and an elevation-dependent weighting strategy is applied to observations at low elevations. For PPP, residual zenith tropospheric delays are estimated every 60 minutes at the reference stations and every 10 minutes at the vessel. For differential positioning, however, they are estimated every 10 minutes at both the reference station and the vessel. Additionally, due to the low data sampling rate at the reference stations in Figure 2, the 1-Hz vessel-borne GPS data were reduced to a 30-second interval.

4 RESULTS AND DISCUSSION

In this section, we assess the accuracy of the satellite clocks and the narrow-lane UPDs determined using the three ring networks, and show the performance comparison between kinematic PPP and differential positioning.

4.1 SATELLITE CLOCK ESTIMATES

Due to the different coverage and sky views of the three ring networks, it is unfair to assess the accuracy of all satellite clock estimates. Hence, only the estimates that are used at the vessel are compared with the truth benchmark, i.e. the CODE final clocks, of which the accuracy in 2004 was better than 0.1 ns (Gendt and Nischan 2005).

Before the comparison, we eliminated the constellation and satellite-dependent offsets between the ring-network-based satellite clocks and the CODE final clocks (Kouba and Springer 2001). The constellation clock offset can be absorbed by receiver clocks, and the satellite-dependent clock offsets can be assimilated into ambiguity estimates (Rocken et al. 2006), thus hardly jeopardizing the PPP solution quality at the vessel. Constellation offsets are removed at each epoch by differencing between a reference clock and all other clocks, and a satellite-dependent offset is removed within each continuous observation session by deducting the mean clock bias. After the removal of both offsets, we used the root mean square (RMS) of the clock differences to quantify the clock accuracy.

For each satellite, all RMS values of the clock differences are better than 0.1 ns, and the three mean RMS values are only 0.041 ns, 0.029 ns and 0.035 ns (Figure 3), respectively, indicating that the accuracy of ring-network-based clocks is very close to that of the CODE final clocks. Moreover, the differences between the three mean RMS values are within ±0.02 ns, but we cannot see any pronounced RMS rise caused by the increasing ring-network radius. This might be because the CODE final clocks are not accurate enough to assess the real accuracy of the ring-network-based clock estimates. However, we can demonstrate that the change of clock accuracy due to the increased ring-network radius up to a few thousand kilometers is smaller than 0.02 ns.

4.2 NARROW-LANE UPD ESTIMATES

For the narrow-lane UPD estimates, we focus on those that are used at the vessel. Due to the lack of any external reference solutions, we chose to assess the relative accuracy between the three sets of estimates. Figure 4 shows the narrow-lane UPD estimates of all observed satellites with respect to PRN03 for the three ring networks. PRN03 is chosen as reference because it was constantly observed during the vessel-borne data collection. Each narrow-lane UPD estimate corresponds to one full pass over a ring network by a satellite pair. The mean formal precision (3σ) of all narrow-lane

UPD estimates for each ring network is about 0.05 cycles. We note that the missing estimates for some ring network, e.g. PRN20 for the small ring, are caused by the insufficient number of reference stations observing the corresponding satellite pair. From Figure 4, we find unexpectedly that, for a satellite pair within one pass, its three independent narrow-lane UPD estimates usually totally differ from each other. Overall, the RMS values of the narrow-lane UPD differences between the three sets of estimates reach up to 0.3 cycles. For this, one explanation is that we used different networks to determine satellite clocks, thus introducing different clock offsets into ambiguity estimates, and consequently obtaining totally different narrow-lane UPD estimates.

Hence, we applied the large-ring-network-based satellite clocks to both the small and medium ring networks to determine their narrow-lane UPDs again. Figure 5 shows the distribution of the new narrow-lane UPD differences between the three sets of estimates. For the three comparisons between the small and the medium, the small and the large, and the medium and the large ring networks, about 84.3%, 65.9% and 75.0% of all narrow-lane UPD differences are within ±0.05 cycles, and about 96.1%, 86.4% and 91.7% are within ±0.1 cycles, respectively (Figure 5). Correspondingly, the RMS values of the new narrow-lane UPD differences are significantly reduced to 0.04 cycles, 0.06 cycles and 0.05 cycles with a mean of only 0.05 cycles, thus confirming the above explanation. More importantly, from Figure 5, the narrow-lane UPD differences between the small and the large rings are clearly larger than those from the other two comparisons, and the differences between the medium and the large ring networks are clearly larger than those between the small and the medium ones. Considering the different coverage of the three ring networks, we demonstrate that the narrow-lane UPD estimates that are used at the vessel are clearly affected by the increased ring-network radius.

Additionally, we indicate that a global, rather than regional, set of UPDs is preferable due to the vast oceanic areas around the world. Actually, global UPDs can be obtained using the method by Ge et al. (2008), which is similar to that of Geng et al. (2009), except for the use of the orbit arc length in the averaging operation.

4.3 COMPARISONS BETWEEN KINEMATIC PPP AND DIFFERENTIAL POSITIONING

Firstly, we compare the positioning accuracy that can be achieved by the kinematic PPP and differential positioning. Table 1 shows the RMS values of the position differences between the truth benchmark and the estimates from the kinematic PPP solutions. We can clearly see that ambiguity resolution reduces the horizontal RMS values to 1-cm level. The East components show larger reductions of 64.7%, 66.7% and 57.9%, whereas the North components of only 37.5%,

36.4% and 23.1% for the three ring networks, respectively. By contrast, the vertical RMS values are around 3 cm after ambiguity resolution. Vertical RMS reductions due to ambiguity resolution are discernable for the medium and large ring networks, but not for the small one, which needs more investigation. Considering the actual accuracy of the truth benchmark, we can deduce that the actual horizontal accuracy for the vessel-borne antenna is at centimeter level and the vertical at sub-decimeter level after ambiguity resolution in the kinematic PPP. Furthermore, the RMS values are enlarged with the increasing ring-network radius. This issue is more pronounced when the ambiguities are not fixed, showing that increasing the ring-network radius affects the positioning accuracy at the vessel.

For comparison, Table 2 shows the RMS values of the position differences between the truth benchmark and the estimates in the kinematic differential solutions. We can see that ambiguity resolution does not reduce the RMS values for the TWTF- and PIMO-based differential positioning. As expected, the RMS values are enlarged with the increasing baseline length, but this enlarging rate is faster than that in Table 1 when ambiguities are fixed. Furthermore, after ambiguity resolution, the RMS values for PPP are smaller than those for differential positioning when the vessel is over a few thousand kilometers away from reference stations. For instance, the RMS values for large-ring-network-based PPP are 55.6%, 56.5% and 13.5% smaller in East, North and Up, respectively, than those for the PIMO-based differential positioning. Considering the use of multiple reference stations and the relatively short baseline lengths for the truth benchmark determination, we believe that the actual accuracy of this benchmark is better than that derived from the BJFS-, TWTF- or PIMO-based differential positioning. Hence, we demonstrate that ambiguity-fixed PPP achieves better positioning accuracy than that of differential positioning when the vessel is over a few thousand kilometers away.

Additionally, for the vessel-borne data, 1-Hz position estimates are of more interests. In this case, differential positioning requires 1-Hz data from reference stations. Nevertheless, for all three ring networks, we can interpolate the above satellite clock estimates at a 1-second interval, and obtain ambiguity-fixed position estimates every 1 s. In this study, if we estimate positions every 5 s in PPP, the resulting RMS values are very close to those in Table 1, and the largest difference is only 0.1 cm.

Secondly, we compare the efficiency of ambiguity resolution between the kinematic PPP and differential positioning. Table 3 shows the number of fixed ambiguities and the number of all ambiguities in PPP and differential positioning. Due to the different definitions for BSD and DD ambiguities, it is not reasonable to directly compare the number of fixed ambiguities or the fixing rates between PPP and differential positioning. Hence, we compare only the change rate of the

number of fixed ambiguities with respect to the increasing network radius or baseline length. Irrespective of the ring-network radius, the number of fixed ambiguities for PPP is almost the same, whereas the number for differential positioning is sharply reduced from 13 to 7 with the increasing baseline length. Hence, we demonstrate that, for ultra long-range kinematic positioning up to a few thousand kilometers, the efficiency of ambiguity resolution for PPP is higher than that for the differential positioning.

Finally, we should indicate that the better performance for PPP than that for differential positioning is attributed to using a ring reference network around the vessel, rather than a single reference station. As a result, more observation information is used in PPP than that in differential positioning. For instance, more than eight carrier phase observations per epoch are available on average at the vessel for all ring networks, whereas only seven are available for BJFS- and TWTF-based differential positioning, and fewer than six for PIMO.

5 CONCLUSIONS

As a potential and promising technique for precise kinematic positioning of remote marine platforms in open oceans, PPP and its ambiguity resolution have been introduced in this study. Three ring networks of reference stations with different radii centered on a vessel were configured to simulate the possible locations of a marine platform in open oceans. We used the three ring networks to independently determine the satellite clocks and UPDs, aiming at assessing the impacts of the ring-network radius on the kinematic PPP performance at the vessel. For comparison, long-range differential positioning based on a single reference station was also used to determine the vessel positions. We attempted three distant reference stations which correspond to the above three ring networks.

For the satellite clocks that are used at the vessel, their accuracy change due to the increased ring-network radius to a few thousand kilometers is smaller than 0.02 ns. Moreover, a high relative accuracy between the three sets of narrow-lane UPD estimates can be achieved if the biases between their corresponding satellite clocks are removed, suggesting that narrow-lane UPDs are closely related to the satellite clocks. More importantly, the narrow-lane UPDs that are used at the vessel are clearly affected by the increasing ring-network radius, but the RMS values of the differences between the three sets of estimates are around 0.05 cycles only.

Ambiguity-fixed PPP can achieve a kinematic positioning accuracy of several centimeters at a remote marine platform. From the comparison between the kinematic PPP and differential positioning, we demonstrate that PPP can achieve both better accuracy of position estimates and higher efficiency of ambiguity resolution when a to-be-positioned marine platform is over a few thousand kilometers away from reference stations. Moreover, the positioning accuracy of PPP at the vessel is affected by the increasing ring-network radius, but the change rate of accuracy is smaller for PPP than that for differential positioning.

Therefore, for the positioning of remote marine platforms in open oceans supporting precise oceanographic and geophysical applications, ambiguity-fixed PPP can achieve an accuracy of several centimeters, even though the distance between the reference network and the platform is up to a few thousand kilometers.

ACKNOWLEDGEMENT

The authors would like to thank the IGS community for data provision and Dr Weiming Tang at Wuhan University for providing the vessel-borne data. Thanks also go to Wuhan University for the provision of PANDA software as collaborative research and development. Two anonymous reviewers are acknowledged for their valuable comments.

REFERENCES

Chadwell CD, Bock Y (2001) Direct estimation of absolute precipitable water in oceanic regions by GPS tracking of a coastal buoy. Geophys Res Lett. 28(19):3701-3704

Chadwell CD, Spiess FN (2008) Plate motion at the ridge-transform boundary of the south Cleft Segment of the Juan de Fuca Ridge from GPS-acoustic data. J Geophys Res. 113, B04415, doi: 10.1029/2007JB004936

Colombo OL, Evans AG, Ando M, Tadokoro K, Sato K, Yamada T (2001) Speeding up the estimation of floated ambiguities for sub-decimetre kinematic positioning at sea. In: Proceedings of ION GNSS 14th International Technical Meeting of the Satellite Division, 11-14 Sep, Salt Lake City, UT, USA

Dach R, Hugentobler U, Fridez P, Meindl M (2007) Bernese GPS software: Version 5.0 manual. Astronomical Institute, University of Bern. 612 pp

Dong D, Bock Y (1989) Global positioning system network analysis with phase ambiguity resolution applied to crustal deformation studies in California. J Geophys Res. 94(B4):3949-3966

Fell P, Maul GA (2000) Marine positioning: state of technology. In: Proceedings of Oceans 2000 MTS/IEEE Conference and Exhibition. 11-14 Sep, Providence, RI, USA

Gagnon K, Chadwell CD, Norabuena E (2005) Measuring the onset of locking in the Peru-Chile trench with GPS and acoustic measurements. Nature. 434:205-208

Ge M, Gendt G, Rothacher M, Shi C, Liu J (2008) Resolution of GPS carrier-phase ambiguities in precise point positioning (PPP) with daily observations. J Geod. 82(7):389-399

Geng J, Teferle FN, Shi C, Meng X, Dodson AH, Liu J (2009) Ambiguity resolution in precise point positioning with hourly data. GPS Solut. 13(4):263-270

Gendt G, Nischan T (2005) 2003/2004 analysis coordinator report. IGS Central Bureau, Pasadena, CA

Grejner-Brzezinska DA, Kashani I, Wielgosz P (2005) On accuracy and reliability of instantaneous network RTK as a function of network geometry, station separation, and data processing strategy. GPS Solut. 9(3):212-225

Griffiths J, Ray JR (2009) On the precision and accuracy of IGS orbits. J Geod. 83(3-4):277-287

Han S, Rizos C (2000) Airborne GPS kinematic positioning and its application to oceanographic mapping. Earth Planets Space. 52(10):819-824

Kato T, Terada Y, Ito K, Hattori R, Abe T, Miyake T, Koshimura S, Nagai T (2005) Tsunami due to the 2004 September 5th off the Kii peninsula earthquake, Japan, recorded by a new GPS buoy. Earth Planets Space. 57(4):297-301

Kouba J, Springer T (2001) New IGS station and satellite clock combination. GPS Solut. 4(4):31-36

Laurichesse D, Mercier F (2007) Integer ambiguity resolution on undifferenced GPS phase measurements and its application to PPP. In: Proceedings of ION GNSS 20th International Technical Meeting of Satellite Division, 25-28 Sep, Fort Worth, TX, USA

Melbourne WG (1985) The case for ranging in GPS-based geodetic systems. In: Proceedings of First International Symposium on Precise Positioning with the Global Positioning System, 15-19 Apr, Rockville, USA

Rivas MB, Maslanik JA, Sonntag JG, Axelrad P (2006) Sea ice roughness from airborne LIDAR profiles. IEEE T Geosci Remote. 44(11):3032-3037

Rocken C, Lukes Z, Mervart L, Johnson J, Iwabuchi T, Kanzaki M (2006) Real-time ionospheric and atmospheric correction for wide area single frequency carrier phase ambiguity resolution. In: Proceedings of ION GNSS 19th International Technical Meeting of the Satellite Division, 26-29 Sep, Fort Worth, TX, USA

Shi C, Zhao Q, Geng J, Lou Y, Ge M, Liu J (2008) Recent development of PANDA software in GNSS data processing. In: Proceedings of the Society of Photographic Instrumentation Engineers, 7285, 72851S. doi: 10.1117/12.816261

Spiess FN, Chadwell CD, Hildebrand JA, Young LE, Purcell GH, Dragert H (1998) Precise GPS/acoustic positioning of seafloor reference points for tectonic studies. Phys Earth Planet In. 108(2):101-112

Teunissen PJG, Kleusberg A (1997) GPS for Geodesy (2nd Edition). Springer-Verlag. 650 pp

Watson CS (2005) Satellite altimeter calibration and validation using GPS buoy technology. Dissertation. University of Tasmania

Zhang X, Andersen OB (2006) Surface ice flow velocity and tide retrieval of the Amery ice shelf using precise point positioning. J Geod. 80(4):171-176

Zhang X, Forsberg R (2007) Assessment of long-range kinematic GPS positioning errors by comparison with airborne laser altimetry and satellite altimetry. J Geod. 81(3):201-211

Zumberge JF, Heflin MB, Jefferson DC, Watkins MM, Webb FH (1997) Precise point positioning for the efficient and robust analysis of GPS data from large networks. J Geophys Res. 102(B3):5005-5017

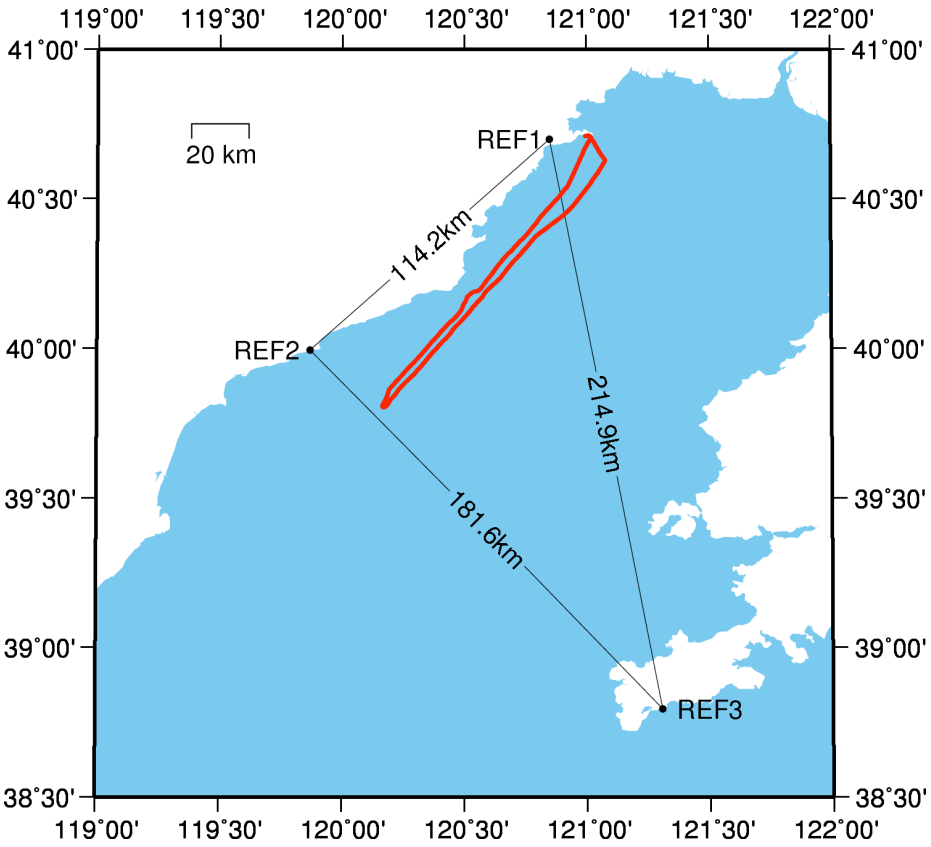

Figure 1 Vessel trajectory in the Bohai Sea of China (red line) and the three 1-Hz reference stations (black dots) used to compute a reference vessel trajectory (truth benchmark)

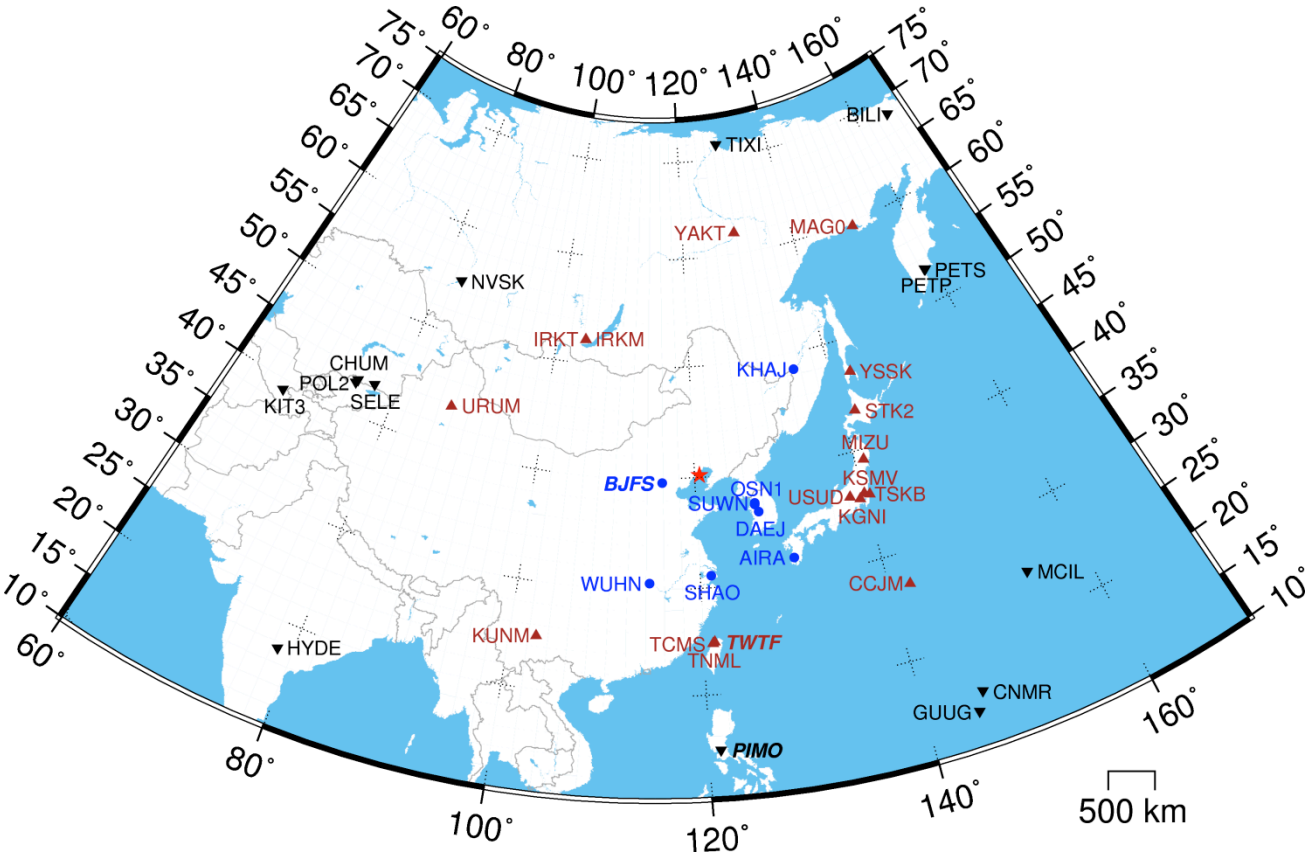

Figure 2 Distribution of reference stations used for the satellite clock and uncalibrated phase delay determination. The red star denotes the approximate position of the vessel. The blue dots, brown triangles and black inverted triangles denote three rings of reference stations centered on the vessel with radii of about 900 km, 2000 km and 3600 km, respectively. For the kinematic differential positioning, three stations with bold italic names, BJFS, TWTF and PIMO, are used as reference stations with distances to the vessel of about 400 km, 1700 km and 2800 km, respectively

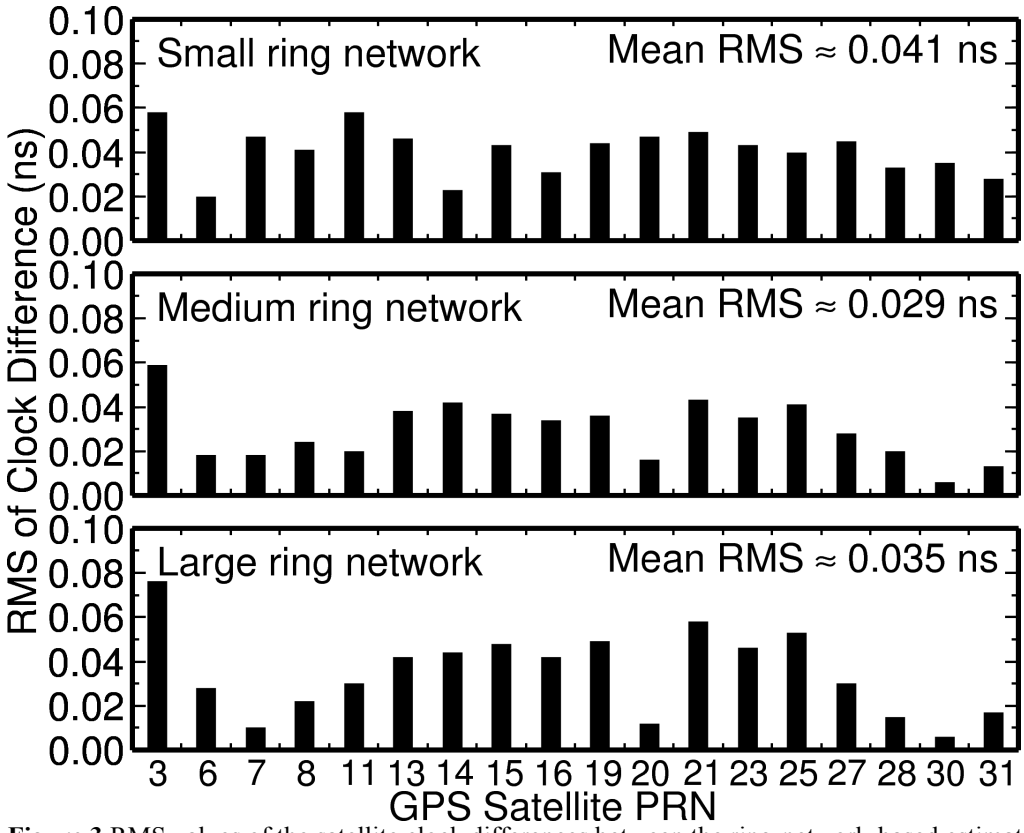

Figure 3 RMS values of the satellite clock differences between the ring-network-based estimates and the CODE final products. Both the constellation and the satellite-dependent offsets have been removed

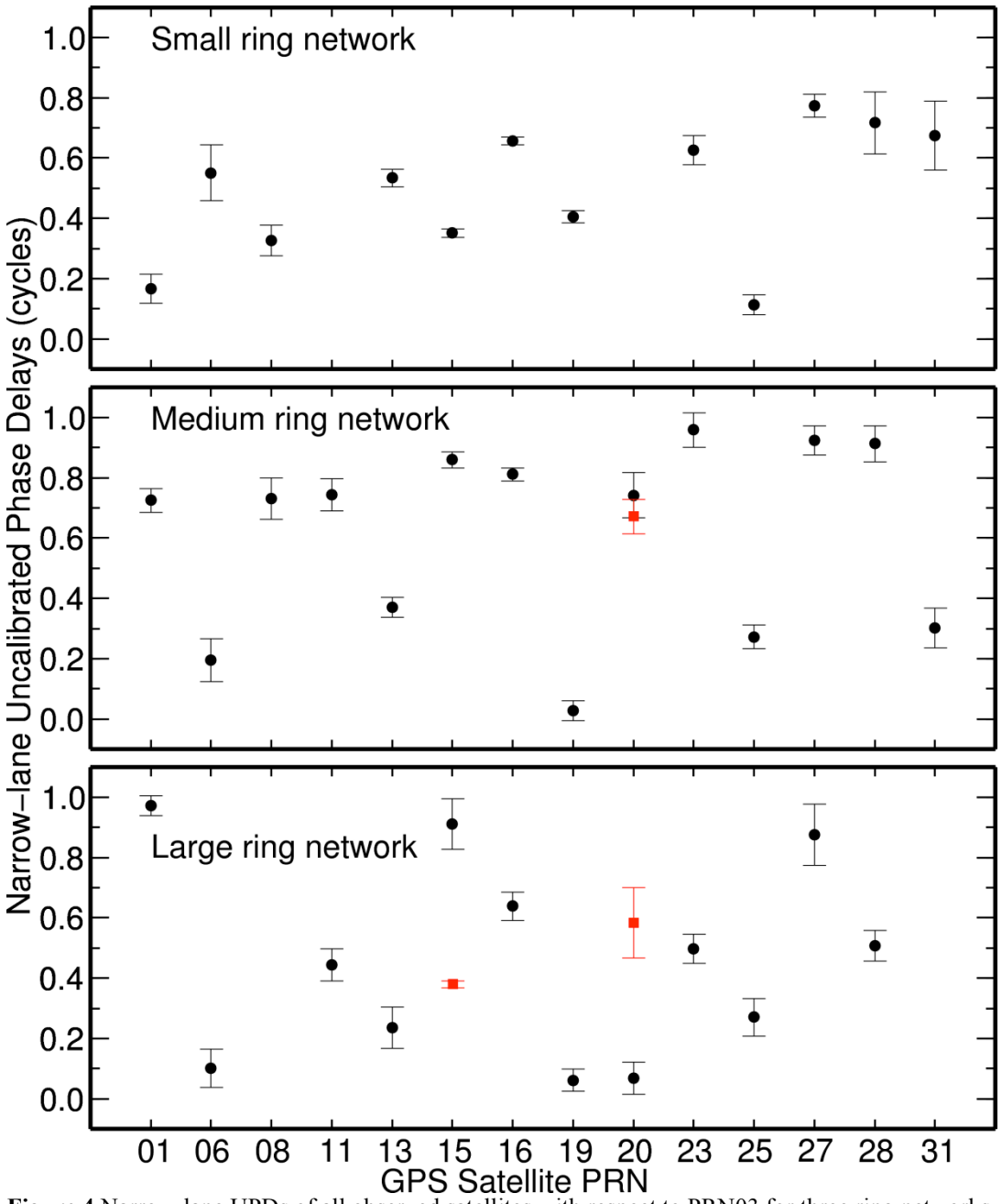

Figure 4 Narrow-lane UPDs of all observed satellites with respect to PRN03 for three ring networks. Each estimate corresponds to one full pass over a ring network by a satellite pair. The solid black circles and red squares denote the estimates for the first and second pass, respectively, whereas the error bars denote the formal precisions of 3σ

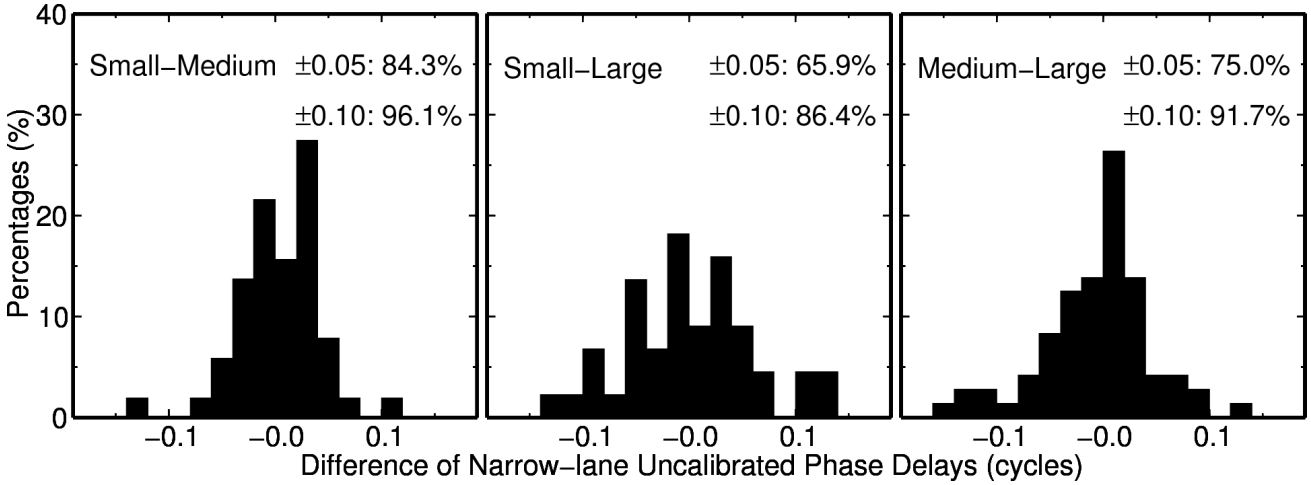

Figure 5 Distribution of narrow-lane UPD differences between the three ring networks when the large-ring-network-based satellite clocks are used in all three ring-network solutions

Table 1 RMS values of the position differences between the truth benchmark and the estimates from the ambiguity-float and ambiguity-fixed kinematic PPP solutions

Reference network	Ring radius (km)	Ambiguity-float (cm)			Ambiguity-fixed (cm)		
		East	North	Up	East	North	Up
Small ring	900	1.7	0.8	1.8	0.6	0.5	2.6
Medium ring	2000	1.5	1.1	3.5	0.5	0.7	2.8
Large ring	3600	1.9	1.3	5.0	0.8	1.0	3.2

Table 2 RMS values of the position differences between the truth benchmark and the estimates from the ambiguity-float and ambiguity-fixed kinematic differential solutions

Reference station	Baseline length (km)	Ambiguity-float (cm)			Ambiguity-fixed (cm)		
		East	North	Up	East	North	Up
BJFS	400	0.7	0.9	2.0	0.5	0.5	1.9
TWTF	1700	0.8	1.5	2.9	0.9	1.7	3.4
PIMO	2800	1.4	2.2	3.5	1.8	2.3	3.7

Table 3 Number of fixed ambiguities (before slash) and number of all ambiguities (behind slash) in PPP and differential positioning

Reference	PPP	Differential positioning
Small-ring/BJFS	14/16	13/19
Medium-ring/TWTF	16/16	13/21
Large-ring/PIMO	16/16	7/16